

# Estimates of the cosmic gamma-ray flux at PeV to EeV energies from the EAS-MSU experiment data

Yu. A. Fomin<sup>1</sup>, N. N. Kalmykov<sup>1</sup>, G. V. Kulikov<sup>1</sup>, V. P. Sulakov<sup>1</sup> and S. V. Troitsky<sup>2,1)</sup>

<sup>1</sup> D.V. Skobeltsyn Institute of Nuclear Physics,

M.V. Lomonosov Moscow State University, Moscow 119991, Russia

<sup>2</sup> Institute for Nuclear Research of the Russian Academy of Sciences,  
60th October Anniversary prospect 7A, 117312 Moscow, Russia

Submitted October 9, 2014

Archival EAS-MSU data are searched for anomalous muonless events which may be caused by primary gamma rays with energies between  $10^{15}$  eV and  $10^{18}$  eV. We consider a refined sample of high-quality data and confirm the previously reported detection of a non-zero gamma-ray flux at  $\sim 5 \times 10^{16}$  eV with a similar flux value but at somewhat lower statistical significance, corresponding to a depletion of the sample. We present upper limits on the flux below and above these energies, including the first constraints in the range  $(10^{17} - 10^{18})$  eV never studied by any other experiment.

Searches for primary gamma rays in the extensive air shower (EAS) data have continued since 1960s (see e.g. Ref. [1] and, for a recent review, Ref. [2]) but started to attract a special attention after the recent announcement of the discovery of high-energy astrophysical neutrinos by the IceCube collaboration [3, 4, 5]. Indeed, in conventional scenarios, the high-energy neutrinos are produced in decays of charged pions, while accompanying neutral pions decay into photons (see e.g. Refs. [6, 7, 8, 9] for more detailed discussions). Discovery of the neutrinos thus gives a hope to find the accompanying photons.

One of the most elaborated methods to discriminate primary gamma rays is to search for air showers with low muon content because secondary muons are produced in hadronic interactions while the photon-induced EAS are mostly electromagnetic. A recent study of EAS-MSU events with estimated number of particles  $N_e > 2 \times 10^7$  has revealed [10] an excess of muonless events compatible with non-zero primary gamma-ray flux at energies  $\gtrsim 50$  PeV. The present work verifies the reported value of the flux with a refined sample of high-quality data and extends the  $N_e$  range to demonstrate a coherent picture of the photon-flux measurements and upper limits in a wide energy band between  $\sim 5$  PeV and  $\sim 500$  PeV.

The EAS-MSU experiment [11] and the analysis method [10] are described in detail in previous works. For the present study, events with the reconstructed number of particles  $N_e > 10^6$  and zenith angles  $\theta < 30^\circ$ , detected in 1982–1990, are selected. Muons with energies  $> 10$  GeV were recorded by the central muon detector of 36.4 m<sup>2</sup> area. For air showers with  $N_e > 10^7$ , the triggering and selection systems have been described in

Ref. [10]. At lower  $N_e$ , the central selection system was used, based on a subset of 7 scintillator detectors; the central one, of 1 m<sup>2</sup> area, and 6 peripheric ones, each of 0.5 m<sup>2</sup> area, located at  $\sim 60$  m from the central one. The trigger corresponds to a simultaneous (within the time gate of 500 ns) firing of the central detector (with the threshold of 1 relativistic particle) and of at least two of peripheric ones (whose thresholds were set at the level of 1/3 of a relativistic particle). It is required that the 3 detectors do not lay on a straight line so that the determination of the EAS arrival direction is possible. The time resolution of the system is  $\sim 5$  ns, which determines the precision of  $\leq 3^\circ$  in the arrival direction. The precision in determination of the core position, important for the present study, is  $\sim 5\%$  of the distance from the shower axis to the installation center, that is does not exceed  $\sim 12$  m even for the farthest events in the sample. The number of particles in a shower is determined by an array of Geiger-Mueller counters with the accuracy of  $\sim 15\%$ .

In each interval in  $N_e$ , the showers in the sample were selected by their core position in such a way that the probability to register an event is not less than 95%. This means that the effective exposure changes with  $N_e$ , though remains constant within every  $N_e$  bin. For the estimates of the integral flux, which require information from several bins, we choose to select constant-exposure subsamples of the available data to exclude the dependence of the result from the assumed gamma-ray spectrum. At  $N_e \geq 2 \times 10^7$ , the outer selection system is used (see Ref. [10]) and the exposure does not change any longer while the  $\geq 95\%$  efficiency is kept. To remove potential instrumental origin of the excess of photon-like events, a careful check of the observation history was

<sup>1)</sup>e-mail: st@ms2.inr.ac.ru

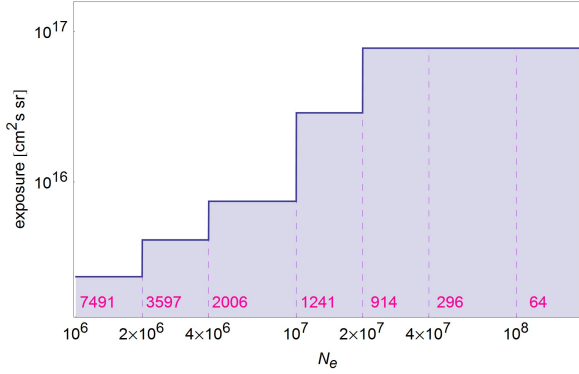


Figure 1. The  $N_e$  dependence of the experiment's exposure. Numbers indicate the total amount of events in the sample within the corresponding  $N_e$  bin.

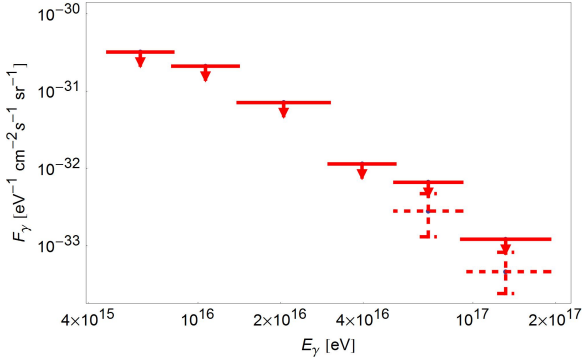


Figure 2. The differential diffuse gamma-ray flux as estimated in this work, see Table 1. Horizontal bars indicate energy bins. For the two highest-energy bins, both 95% CL upper limits and 68% CL error bars are shown.

performed and the days with any irregularities, such as a detector failure, were removed from the sample. This reduces the exposure at large  $N_e$  by  $\sim 1/3$  as compared to the previous study. The exposure as a function of  $N_e$  is presented in Fig. 1.

An event is considered a photon candidate if the 36.4 m<sup>2</sup> muon detector located in the array's center did not record any signal. These muonless showers, however, may be rarely produced by primary hadrons. The method to estimate the expected background of muonless events from hadronic showers was described in detail in Ref. [10]. It includes simulations of artificial proton-induced showers by means of the AIRES 2.6.0 [12] package with the QGSJET-01 [13] hadronic interaction model.

The results of the bin-by-bin study are presented in Table 1 and Fig. 2 while the estimate of the integral gamma-ray flux is given in Table 2 and compared to results of other experiments in Fig. 3. The latter plot presents also a comparison with an example theoretical

$N_e$ , $10^6$	$E_\gamma$ , PeV	$N_{\text{obs}}$	$N_{\text{exp}}$	$10^{32}F_\gamma$ , (eV cm <sup>2</sup> s sr) <sup>-1</sup>
1 – 2	4.7 – 8.1	17	34.0	<32
2 – 4	8.1 – 14	7	8.7	<21
4 – 10	14 – 30	3	3.8	<3.9
10 – 20	30 – 52	5	4.0	<1.14
20 – 40	52 – 91	25	16.5	<0.660
40 – 100	91 – 190	4	0.5	<0.121
				$0.046^{+0.036}_{-0.022}$

Table 1. Estimates of the differential diffuse gamma-ray flux.  $E_\gamma$  is the mean energy of a primary photon which produces an EAS with the corresponding  $N_e$ ;  $N_{\text{obs}}$  is the number of observed muonless events in the bin;  $N_{\text{exp}}$  is the expected number of background muonless events from usual cosmic rays;  $F_\gamma$  is the estimate of the differential gamma-ray flux in the bin. It does not depend on the assumed photon spectrum because the exposure is constant within a bin.

$N_e^{\text{min}}$ , $10^6$	$E_\gamma^{\text{min}}$ , PeV	$N_{\text{obs}}$	$N_{\text{exp}}$	$10^{16}I_\gamma$ , (cm <sup>2</sup> s sr) <sup>-1</sup>
1	4.7	19	34.0	< 12
2	8.1	8	8.0	<16
4	14	4	4.5	< 7.1
10	30	6	4.3	< 2.9
20	52	29	17.0	< 3.1
				$1.55^{+0.75}_{-0.67}$
40	91	4	0.5	<1.20
				$0.45^{+0.36}_{-0.21}$
100	190	0	< 0.001	<0.40

Table 2. Estimates of the integral diffuse gamma-ray flux  $I_\gamma$  at photon energies above  $E_\gamma^{\text{min}}$ , corresponding to  $N_e > N_e^{\text{min}}$ .

curve from Ref. [9] normalized to the IceCube neutrino flux. All upper limits reported in the tables and plots are 95% confidence level (CL). Wherever a measurement with error bars is presented, the error bars are 68% CL, statistical only.

Several comments to these results are in order.

1. The excess of muonless events at  $N_e \gtrsim 10^7$  suggests [10, 25] a nonzero gamma-ray flux at several dozen PeV. In this work, we used a refined sample of high-quality data and obtained a value of the flux in excellent agreement with the result reported in [10]. The statistical significance of this result is reduced in accordance

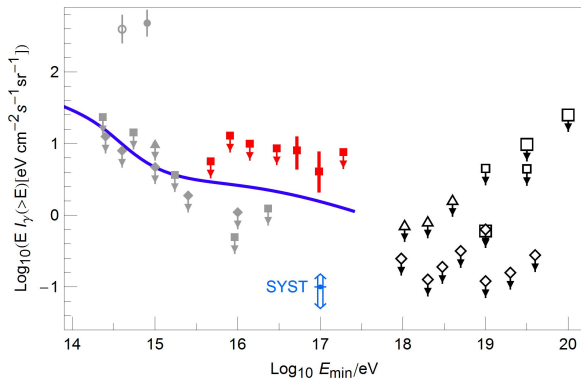


Figure 3. Estimates of the integral gamma-ray flux from EAS-MSU (dark (red) squares and error bars; this work) and from other experiments: gray symbols – open circle (Tien Shan [14], detection claim), circle (Lodz [15], detection claim), triangles (EAS-TOP [16]), squares (CASA-MIA [17]), diamonds (KASCADE [18, 19]); black open symbols – triangles (Yakutsk [20]), diamonds (Pierre Auger [21, 22]), small squares (AGASA [23]), large squares (Telescope Array [24]). Systematic uncertainties (estimated for EAS-MSU but relevant for other data as well, see text) are shown by a double arrow. The curve represents a theoretical prediction of Ref. [9] for the model in which photons and neutrinos are produced in cosmic-ray collisions with the hot gas surrounding our Galaxy, assuming the best-fit IceCube observed neutrino spectrum.

with the reduction in the used exposure by  $\sim 1/3$ . Note that the precise photon energy to which the flux corresponds is slightly different from the previous work due to more accurate estimates of  $N_e$  for gamma-ray showers (the change is within the systematic uncertainties). The excess is not seen at lower energies thus giving additional support to its physical, and not instrumental, origin. At energies above  $\sim 10$  PeV, where the exposure is still low, the excess starts to build up but its significance is low. Therefore, the analysis carried out in several energy bins results in a coherent picture supporting the first ever observation of cosmic gamma rays above 100 TeV with a relatively hard spectrum.

2. As it was discussed in Ref. [10], the dominant source of systematic errors for this kind of a study is related to the background estimation: various models of hadronic interactions predict different muon content of air showers; additional uncertainty is related to the chemical composition of the bulk of primary cosmic rays. The resulting systematic error of the derived gamma-ray flux is  $\pm 50\%$  for the EAS-MSU data [10], and a similar scale of uncertainties is expected for other experiments whose results are presented in Fig. 3. At lower energies of order a few PeV, the observed number

of muonless events is significantly lower than predicted in our simulations, see Table 1. The most probable reason for that is the assumption of pure proton composition in the estimation of the background of muonless events. With the realistic composition, the number of muon-rich showers increases, thus reducing the background. We however choose to keep the conservative high background for the detection claim in higher energy bins and postpone a detailed estimate of the effect of the realistic composition to a future work. The undercount of muonless events at PeV energies is unlikely to be related to the excess of muons in air showers with respect to simulations, as observed by the Yakutsk [27] and Pierre Auger [28, 29] experiments at much higher primary energies but for lower-energy muons.

3. The constraints presented here for energies  $\sim (10^{17} - 10^{18})$  eV cover the region unexplored by other experiments and present therefore the first ever published limits on the diffuse gamma-ray flux at these energies. These limits may be improved, or non-zero photon flux observed, by future experiments like Tunka-HiSCORE [30] or low-energy extensions of the Telescope Array (TALE [31]) and Pierre Auger (AMIGA [32]) experiments, as well as in reanalysis of archival data of muon detectors in Yakutsk [33]. Additional tests of the origin of the (50–100) PeV excess of muonless events in the EAS-MSU data will be provided by a dedicated study of other EAS observables which is currently under way.

We are indebted to Grigory Rubtsov for interesting and useful discussions and to Oleg Kalashev for sharing the results of Ref. [9] prior to publication. The experimental work of the EAS-MSU group and computer simulations were supported in part by the grants of the Government of the Russian Federation (agreement 14.B25.31.0010) and of the Russian Foundation for Basic Research (projects 14-02-00372 and 13-02-00214). Development of the methods to search for primary photons and application of these methods to the EAS-MSU data were supported by the Russian Science Foundation, grant 14-12-01340.

- 
1. G.B. Khristiansen, G.V. Kulikov, Yu.A. Fomin, *Ultra-high-energy cosmic radiation*, Moscow, Atomizdat, 1975.
  2. M. Risse and P. Homola, *Mod. Phys. Lett. A* **22** (2007) 749 [astro-ph/0702632].
  3. M. G. Aartsen *et al.* [IceCube Collaboration], *Phys. Rev. Lett.* **111** (2013) 021103 [arXiv:1304.5356 [astro-ph.HE]].

4. M. G. Aartsen *et al.* [IceCube Collaboration], *Science* **342** (2013) 6161, 1242856 [arXiv:1311.5238 [astro-ph.HE]].
5. M. G. Aartsen *et al.* [IceCube Collaboration], *Phys. Rev. Lett.* **113** (2014) 101101 [arXiv:1405.5303 [astro-ph.HE]].
6. N. Gupta, *Astropart. Phys.* **48** (2013) 75 [arXiv:1305.4123 [astro-ph.HE]].
7. L. A. Anchordoqui, H. Goldberg, M. H. Lynch, A. V. Olinto, T. C. Paul and T. J. Weiler, *Phys. Rev. D* **89** (2014) 083003 [arXiv:1306.5021 [astro-ph.HE]].
8. M. Ahlers and K. Murase, *Phys. Rev. D* **90** (2014) 023010 [arXiv:1309.4077 [astro-ph.HE]].
9. O. E. Kalashev and S. V. Troitsky, arXiv:1410.2600.
10. Yu. A. Fomin, N. N. Kalmykov, G. V. Kulikov, V. P. Sulakov and S. V. Troitsky, *J. Exp. Theor. Phys.* **117** (2013) 1011 [arXiv:1307.4988 [astro-ph.HE]].
11. S. N. Vernov, G. B. Khristiansen, V. B. Atrashkevich *et al.*, *Bull. Russ. Acad. Sci. Phys.* **44** (1980) 80 [*Izv. Ross. Akad. Nauk Ser. Fiz.* **44** (1980) 537].
12. S.J. Sciutto, *AIRES: A system for air shower simulations. Version 2.6.0*, 2002.
13. N. N. Kalmykov, S. S. Ostapchenko and A. I. Pavlov, *Nucl. Phys. Proc. Suppl.* **52B** (1997) 17.
14. S. I. Nikolsky, I. N. Stamenov and S. Z. Ushev, *J. Phys. G* **13** (1987) 883.
15. J. Gawin, R. Maze, J. Wdowczyk and A. Zawadzki, *Canad. J. Phys.* **46** (1968) 75.
16. M. Aglietta, B. Alessandro, P. Antoni *et al.* [EAS-TOP Collaboration], *Astropart. Phys.* **6** (1996) 71.
17. M. C. Chantell, C.E. Covault, J.W. Cronin *et al.* [CASA-MIA Collaboration], *Phys. Rev. Lett.* **79** (1997) 1805 [astro-ph/9705246].
18. G. Schatz, F. Fessler, T. Antoni *et al.* [KASCADE collaboration], *Proc. 28th ICRC, Tsukuba* **4** (2003) 2293.
19. J. Alvarez-Muniz *et al.* EPJ Web Conf. **53** (2013) 01009 [arXiv:1306.4199 [astro-ph.HE]].
20. A. V. Glushkov, I. T. Makarov, M. I. Pravdin *et al.*, *Phys. Rev. D* **82** (2010) 041101 [arXiv:0907.0374 [astro-ph.HE]].
21. J. Abraham, P. Abreu, M. Aglietta *et al.* [Pierre Auger Collaboration], *Astropart. Phys.* **29** (2008) 243 [arXiv:0712.1147 [astro-ph]].
22. P. Abreu, M. Aglietta, E.J. Ahn *et al.* [Pierre Auger Collaboration], arXiv:1107.4805 [astro-ph.HE].
23. K. Shinozaki, M. Chikawa, M. Fukushima *et al.* [AGASA Collaboration], *Astrophys. J.* **571** (2002) L117.
24. T. Abu-Zayyad, R. Aida, M. Allen *et al.* [Telescope Array Collaboration], *Phys. Rev. D* **88** (2013) 11, 112005 [arXiv:1304.5614 [astro-ph.HE]].
25. N. Kalmykov, J. Cotzomi, V. Sulakov *et al.*, *Izv. Ross. Akad. Nauk Ser. Fiz.* **75** (2009) 584.
26. N. N. Kalmykov, G. V. Kulikov, V. P. Sulakov and Yu. A. Fomin. Talk at the Russian Cosmic-Ray Conference, August 2014.
27. A. V. Glushkov, I. T. Makarov, M. I. Pravdin *et al.*, *JETP Lett.* **87** (2008) 190 [arXiv:0710.5508 [astro-ph]].
28. R. Engel [Pierre Auger Collaboration], arXiv:0706.1921 [astro-ph].
29. A. Aab *et al.* [Pierre Auger Collaboration], arXiv:1408.1421 [astro-ph.HE].
30. M. Tluczykont, D. Hampf, U. Einhaus *et al.*, *AIP Conf. Proc.* **1505** (2012) 821.
31. S. Ogio *et al.* [Telescope Array Collaboration], Talk at the International Symposium on Future Directions in UHECR Physics, CERN, 13-16 February 2012.
32. A. Etchegoyen [Pierre Auger Collaboration], arXiv:0710.1646 [astro-ph].
33. L. G. Dedenko, G. F. Fedorova, T. M. Roganova *et al.*, *J. Phys. G* **39** (2012) 095202.